Robotica (2002) volume 20, pp. 359–366. © 2002 Cambridge University Press
DOI: 10.1017/S026357470100337X Printed in the United Kingdom

Calibration-based absolute localization of parts for multi-robot assembly

Edward J. Park, Weihua Xu and James K. Mills

Laboratory for Nonlinear Systems Control, Department of Mechanical and Industrial Engineering, University of Toronto, 5 King's College Road, Toronto, Ontario (Canada) M5S 3G8

(Received in Final Form: February 1, 2001)

SUMMARY

In multi-robot assembly of parts, for successful mating, the grasped parts must be located with sufficiently small position and orientation errors so that assembly can be achieved. This paper describes a new approach for determining the absolute three-dimensional spatial location of parts grasped by robots during assembly. Through a combination of robot pose calibration and part-sensor calibration, the robot, used to grasp the part, is calibrated to accurately position and orient parts to a designated mating location. First, by employing a robot pose measurement system, the 6 DOF robot pose errors relative to a reference coordinate frame are compensated. Second, with the implementation of a part pose measurement, the 6 DOF part pose errors, relative to the robot tool frame, are estimated in real time. An experimental verification of the proposed methodology using a single FANUC S–110 robot manipulating an automotive sheet metal part is described.

KEYWORDS: Multi-robot assembly; Part localization; Robot calibration; Laser sensor.

1. INTRODUCTION

The underlying motivation for this work is the development of assembly technology to eliminate hardware fixtures currently in use in many assembly processes. The state of the art approach to high-volume manufacturing assembly processes typically makes use of product-dedicated, custom-designed hardware fixtures. The function of these fixtures is to accurately locate and immobilize the parts, and also to align the parts with respect to each other so they can be bonded together. However, fixtures are very costly and require long lead-times to design, manufacture, and install. They reduce manufacturing flexibility because they must be modified or redesigned whenever the size or shape of parts assembled is changed. One solution to these inherent drawbacks is the replacement of dedicated fixtures by multiple robots that can quickly be reprogrammed to accommodate part changes.[1]

For example, a typical multi-robot assembly operation may consist of the following operations: two robots each grasp one part, correctly position and orient the parts for mating, and then a third robot used to weld the two parts together, forming an assembly. Assemblies comprised of more than two parts are assembled through repeated application of this process. However, to reduce the cost of this process, parts are presented to the robots with low accuracy part holders. Approximate initial locations of the parts are known, since the uncertainty in location of the parts, when placed in a part holder, is 5%–10% of the dimensions of the parts. Grasping, herein referred to as "mis-located" parts, results in misalignment between the parts when they are brought together by the two robots, and renders the subsequent bonding operation by a robot welder unsuccessful. For successful assembly, the parts, once grasped, must be localized, in both position and orientation, within required tolerances for assembly. The assembly tolerances are substantially less than that of the part-holder.

Consider two parts, denoted part A and part B, grasped by robot A and robot B, respectively. These parts are to be mated by the robots for assembly. One solution to the above assembly problem is to find relative misalignments between the two parts with respect to each other prior to the mating, i.e., Kim and Cho,[2] and move the robots to correct the misalignments. Another solution to the problem is to determine the absolute locations of both parts with respect to a known reference frame. In the latter approach, pursued in this paper, two problems must be addressed in order to successfully assemble the two parts.

The first is the precise movement of the robot A (B), while grasping part A (B), to a specified location where the two parts are mated. This is called the robot calibration problem. Note that to precisely move either robot to a designated location, the accuracy and repeatability of the robot should be substantially better than the required tolerance for the assembly process. To address the first problem, a robot pose measurement system for robot calibration, developed by Xu and Mills,[3] is used. Its measurement method, which is an extension of robot repeatability measurement methods that employ a test block and six dial gauges,[4] uses a specially designed mechanical fixture containing three digital dial gauges. This enables the measurement of complete pose industrial robots. This measurement system is relatively low-cost, easy to use, and provides sufficiently accurate calibration results for the purposes of our work.

The second problem lies in determining the accurate pose of part A (B) with respect to the tool frame of the robot A (B). This is a relative part localization problem. As discussed, when the robot grasps the part from a part holder, the precise location of the part is unknown, and hence must

https://doi.org/10.1017/S026357470100337X Published online by Cambridge University Press

be determined. To address this problem, we extend the direct calibration localization method, proposed by Murray and Pohlhammer.[5] In addition, a part pose measurement system introduced by Park and Mills[6] is employed. This measurement system, which utilizes laser based proximity and edge sensors, extracts the part feature data in real-time. The direct calibration method can also be referred to as "part-sensor calibration," since it determines the relationship between the part pose data and the sensor measurement data in robot tool coordinates, through a calibration procedure. By combining the robot calibration and part-sensor calibration processes into a single procedure, the entire assembly system can be calibrated for the required assembly tasks, and thus absolute localization of parts can be achieved. In other words, this means that the parts can be localized relative to any world coordinate frame defined by the user of the robot.

Specifically, we examine the assembly of thin-walled sheet metal parts, used in automotive bodies, as an illustrative example in our work. Note that as a first step in the ongoing research on multi-robot assembly, the robot and part pose measurement systems test-bed constructed here involve a single 6 degree-of-freedom (DOF) FANUC S–110 industrial robot. While these systems are specific to the assembly of automotive sheet metal parts (i.e., automotive front quarter panel), the theory and results presented here may be applied to other multi-robot assembly tasks.

This work represents the first reported work that addresses the absolute three-dimensional (3-D) localization problem of thin-walled parts in assembly. This paper is organized as follows. In the next section, the general 3-D absolute part localization problem is described in detail. In Section 3, the robot pose measurement technique is described. Similarly, in Section 4, the part pose measurement algorithm is presented, which is followed in Section 5 by experimental results of a single FANUC S–110 robot manipulating an automotive fender on the test-bed. Finally, Section 6 concludes the work.

2. PROBLEM DESCRIPTION

2.1. Coordinate System description

In this section, we define the coordinate systems, which are used for the absolute part localization. As shown in Figure 1, the base frame *b-xyz* is assigned inside the base of the robot. For instance, the base frame origin of the FANUC S–110 robot is located at the intersection of the first and second joint axes. The world frame *w-xyz* is defined at an arbitrary location in the robot workspace. The tool frame *t-xyz* is affixed to tools held rigidly by the robot: (i) a tooling ball used for robot calibration and (ii) a part gripper used for part-sensor calibration. For both the tooling ball and the gripper, the tool frame is defined at the same location with respect to the robot end-effector frame – at the center point of the tooling ball. As shown in Figure 1, the z axis of the tool frame is in the normal vector direction of the faceplate of the end-effector, with the x and y axes in arbitrary directions parallel to the faceplate. The part frame *p-xyz* is attached to the part. The part-holder frame, *1-xyz*, represents the location from which the robot picks up or grasps the part. The part mating frame, *2-xyz*, represents the desired mating location to which the robot is to move the part. To assemble the parts, through the part-sensor calibration and the robot calibration, the part frame *p-xyz* and the tool frame *t-xyz* are located coincident with the part mating frame, *2-xyz*.

2.2. Absolute Part Localization Problem

Consider a part, manually placed into a part-holder. Since the part holder is not a precision device, the part is not placed in the same location every time, but arbitrarily placed, close to the correct location in the robot workspace. The robot will grasp the part at the partholder frame to within the repeatability error of the robot. However since the part is arbitrarily placed, the part pose (position and orientation), is not known precisely with respect to the tool

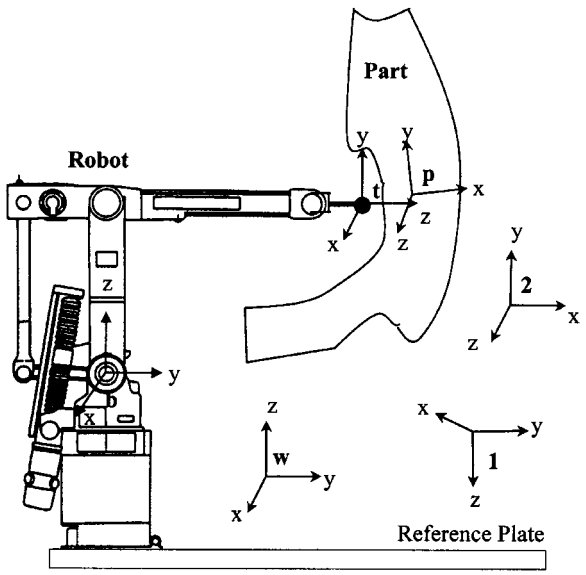


Fig. 1. Definition of coordinate systems for absolute part localization (*t-xyz*: tool frame, *p-xyz*: part frame, *b-xyz*: base frame, *w-xyz*: world frame, 1-*xyz*: part-holder frame, 2-*xyz*: part mating frame).

https://doi.org/10.1017/S026357470100337X Published online by Cambridge University Press

frame or any other frame. Thus, the grasped part cannot be mated properly with other parts unless the actual pose of the part is determined and the part is relocated accordingly.

Figure 2 shows a schematic depicting the absolute part localization problem. As discussed, ideally, the part frame *p-xyz* and the tool frame *t-xyz* should be coincident with the part mating frame, *2-xyz*. The dotted line represents the part at the part mating frame in the robot workspace. The dashed line shows the mis-located part, due to the inaccuracy (pose error) introduced by robot. The solid line represents the mis-located part due to both the robot pose error and the part pose error caused by pose uncertainty, arising from grasping the part from a part-holder. Absolute part localization allows the robot to correct the pose of the mis-located part to the desired location, the part mating frame *2-xyz*, for subsequent mating. Using both robot calibration and the part-sensor calibration, the robot pose error and the part pose error are determined, respectively. With these data, compensation for the part mis-location can be achieved.

Generally, the localization of a part is a 6 DOF problem: determination of three position variables (x, y, z) and three orientation variables (w, p, r) with respect to a known reference frame. Let $\Delta\mathbf{L}^p \in \Re^{1\times 6}$ represent the complete 6 DOF pose error of the part, i.e.,

$$\Delta\mathbf{L}^p = [\Delta x \quad \Delta y \quad \Delta z \quad \Delta w \quad \Delta p \quad \Delta r]. \tag{1}$$

Similarly, let $\Delta\mathbf{L}^r \in \Re^{1\times 6}$ represent the complete pose error of the robot, i.e.,

$$\Delta\mathbf{L}^r = [\Delta X \quad \Delta Y \quad \Delta Z \quad \Delta W \quad \Delta P \quad \Delta R]. \tag{2}$$

Then the mis-location of the part is given by a 1×6 vector

$$\Delta\mathbf{L} = \Delta\mathbf{L}^r + \Delta\mathbf{L}^p. \tag{3}$$

Hence, $-\Delta\mathbf{L}$ is the amount by which the tool frame must move from the current location to compensate for the mis-location due to the robot and part pose errors. Note that $\Delta\mathbf{L}^r$, $\Delta\mathbf{L}^p$ and $\Delta\mathbf{L}$ are defined relative to the part mating frame *2-xyz*.

3. ROBOT POSE ERROR ESTIMATION

In order to achieve absolute localization of the part, the absolute location of the robot must be calibrated. Assume that the uncalibrated robot has sufficiently low repeatability error, but insufficient accuracy, to move the part to a designated location in the workspace. In this section, the robot pose measurement technique[3] for estimating robot pose error $\Delta\mathbf{L}^r$ is presented.

The FANUC S–110 robot is controlled by a KAREL R-F controller, which is capable of displaying the current robot pose information of the tool frame *t-xyz* with respect to the base frame *b-xyz*, or a coordinate frame defined by the user. Using the KAREL software or a teach pendant, the tool frame can be redefined to a specified location, such as pose "i", by designating the desired pose variables: (X_i Y_i Z_i W_i P_i R_i). With this information, the 4×4 desired transformation matrix, which expresses the desired coordinate transformation from the base frame to the tool frame of pose "i", can be expressed as follows

$${}^b_i\mathbf{T}^d = \begin{bmatrix} {}^b_i\mathbf{R}^d & {}^b_i\mathbf{p}^d \\ 0 & 1 \end{bmatrix} \tag{1}$$

where:

$${}^b_i\mathbf{R}^d = \begin{bmatrix} \cos R_i & -\sin R_i & 0 \\ \sin R_i & \cos R_i & 0 \\ 0 & 0 & 1 \end{bmatrix} \begin{bmatrix} \cos P_i & 0 & \sin P_i \\ 0 & 1 & 0 \\ -\sin P_i & 0 & \cos P_i \end{bmatrix} \begin{bmatrix} 1 & 0 & 0 \\ 0 & \cos W_i & -\sin W_i \\ 0 & \sin W_i & \cos W_i \end{bmatrix} \tag{2}$$

and

$${}^b_i\mathbf{p}^d = [X_i \quad Y_i \quad Z_i]^T \tag{3}$$

where ${}^b_i\mathbf{R}^d$ is the 3×3 rotation matrix from the base frame to the tool frame of pose "i" and ${}^b_i\mathbf{p}^d$ is the 3×1 position vector of the tool frame with respect to the base frame, all for $i = 1, \ldots, N$. When the robot moves from pose "1" (the part pick up location) to pose "2" (the part mating location), as shown in Figure 3, the desired transformation matrix from poses "1" to "2" is given by

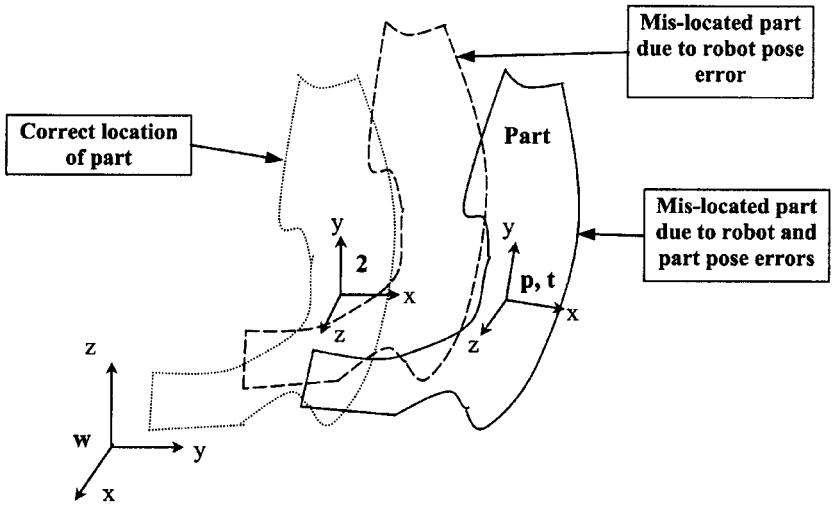


Fig. 2. Absolute part localization problem (*2-xyz*: part mating frame, *t-xyz*: tool frame, *p-xyz*: part frame).

https://doi.org/10.1017/S026357470100337X Published online by Cambridge University Press

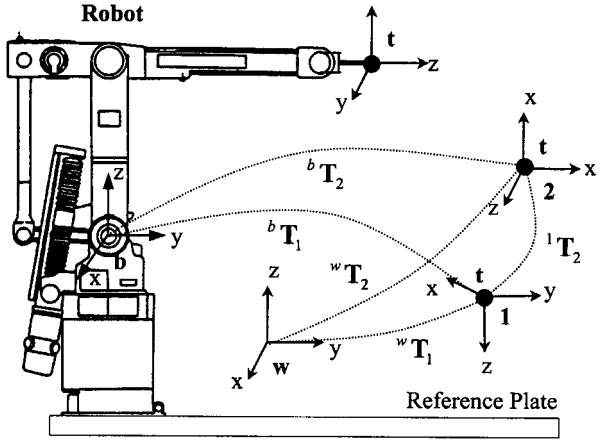


Fig. 3. Robot pose estimation.

$$ {}^{1}_{2}\mathbf{T}^{d} = {}^{b}_{1}\mathbf{T}^{\,d}\,{}^{b}_{2}\mathbf{T}^{d} = \begin{bmatrix} {}^{1}_{2}\mathbf{R}^{d} & {}^{1}_{2}\mathbf{p}^{d} \\ 0 & 1 \end{bmatrix} \tag{4} $$

where ${}^{u}\mathbf{T}^{d}_{1}$, and ${}^{u}\mathbf{T}^{d}_{2}$ are the desired transformation matrices from the user frame to the poses "1" and "2" respectively; ${}^{1}_{2}\mathbf{R}^{d}$ and ${}^{1}_{2}\mathbf{p}^{d}$ are the desired rotation matrix and position vector from the poses "1" to "2", respectively.

Similarly, the 4×4 actual transformation matrix, which is measured from the world frame to the tool frame, of pose "i", is given by

$$ {}^{w}_{i}\mathbf{T}^{a} = \begin{bmatrix} {}^{w}_{i}\mathbf{R}^{a} & {}^{w}_{i}\mathbf{p}^{a} \\ 0 & 1 \end{bmatrix} \tag{5} $$

where ${}^{w}_{i}\mathbf{R}^{a}$ is the 3×3 rotation matrix from the world frame to the tool frame of pose "i" and ${}^{w}_{i}\mathbf{p}^{a}$ is the 3×1 position vector of the tool frame with respect to the world frame, all for $i=1, \ldots, N$. Then the transformation from the poses "l" to "2" is given by

$$ {}^{1}_{2}\mathbf{T}^{a} = {}^{w}_{1}\mathbf{T}^{a}\,{}^{w}_{2}\mathbf{T}^{a} = \begin{bmatrix} {}^{1}_{2}\mathbf{R}^{a} & {}^{1}_{2}\mathbf{p}^{a} \\ 0 & 1 \end{bmatrix} \tag{6} $$

where ${}^{w}_{1}\mathbf{T}^{a}$ and ${}^{w}_{2}\mathbf{T}^{a}$ are the transformation matrices from the world frame to the poses "1" and "2" respectively; ${}^{1}_{2}\mathbf{R}^{a}$ and ${}^{1}_{2}\mathbf{p}^{a}$ are the rotation matrix and position vector from the poses "1" and "2", respectively. Note that the quantities ${}^{w}_{i}\mathbf{R}^{a}$ and ${}^{w}_{i}\mathbf{p}^{a}$, are obtained by using the robot pose measurement system shown in Figure 4. See Xu and Mills[3] for the description of the complete measurement procedures.

Finally, the accuracy of the robot can be evaluated by comparing ${}^{1}_{2}\mathbf{T}^{d}$ and ${}^{1}_{2}\mathbf{T}^{a}$, i.e.,

$$ \Delta^{1}_{2}\mathbf{R} = {}^{1}_{2}\mathbf{R}^{d} - {}^{1}_{2}\mathbf{R}^{a} = \begin{bmatrix} u_{11} & u_{12} & u_{13} \\ u_{21} & u_{22} & u_{23} \\ u_{31} & u_{32} & u_{33} \end{bmatrix} \tag{7} $$

$$ \Delta^{1}_{2}\mathbf{p} = {}^{1}_{2}\mathbf{p}^{d} - {}^{1}_{2}\mathbf{p}^{a} = [\Delta X \quad \Delta Y \quad \Delta Z]^{T}. \tag{8} $$

Now, to express equation (7) in the form of equation (2), in roll, pitch and yaw angles, we compute the following from equation (7):[7]

$$ \begin{aligned} \Delta R &= \tan^{-1}\left(u_{32} \Big/ u_{33} \right) \\ \Delta P &= \tan^{-1}\left(-u_{31} \Big/ \sqrt{u_{11}^2 + u_{21}^2} \right) \\ \Delta W &= \tan^{-1}\left(u_{21} \Big/ u_{11} \right). \end{aligned} \tag{9} $$

Substituting equations (8) and (9) into equation (2), the robot pose error $\Delta\mathbf{L}^{r}$ relative to the desired mating location (*2-xyz*) is obtained. In the above equations, the actual pose of the robot, which is measured from the world frame.

4. PART POSE ERROR ESTIMATION

In order to achieve absolute localization of the part, the pose of the part with respect to the robot must be determined. In this section, the part pose measurement technique[6] for estimating part pose error $\Delta\mathbf{L}^{p}$ is presented.

The part pose error $\Delta\mathbf{L}^{p}$, is determined through the use of a number of spatially distributed sensors. For sufficiently accurate 6 DOF localization of thin-walled sheet metal parts, both thin-edges and surfaces must be detected. Herein, we employ a set of seven laser beam sensors, each providing a single measurement point on the part: three points on the top surface using proximity sensors and four points around the edges using edge sensors. The sensors are placed in a configuration shown in Figure 5. Now, let $\mathbf{S} \in \Re^{1\times7}$ be defined as:

$$ \mathbf{S} = [s_1 \quad s_2 \quad s_3 \quad s_4 \quad s_5 \quad s_6 \quad s_7] \tag{10} $$

where s_i, $i=1, \ldots, 4$ correspond to the outputs from proximity sensors and s_i, $i=5, \ldots, 7$, to edge sensors, expressed with respect to each sensor local coordinate frame.

Figure 5 illustrates the relative placement of each measurement point and sensor coordinate frame with respect to the part. Note that the measurement points are widely distributed over the surface and the edges. Sensor s_7 is a redundant sensor, in order to achieve better part pose estimation accuracy.

https://doi.org/10.1017/S026357470100337X Published online by Cambridge University Press

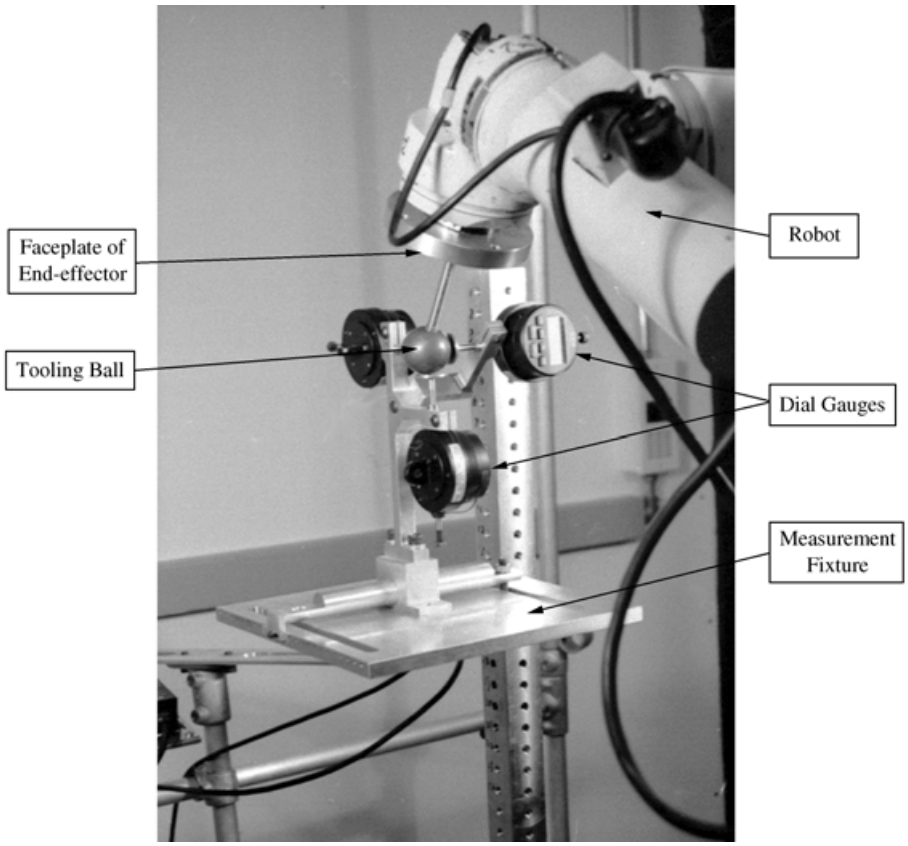


Fig. 4. Robot pose measurement system.

The algorithm presented in this section determines the actual part pose with respect to the tool frame, *t-xyz*, shown in Figure 5. The algorithm is based on the direct calibration method[5], which is comprised of two procedures: (i) computation of the correspondence – called mappings herein – between the part pose errors $\Delta\mathbf{L}^p$ and sensor measurements **S**, and (ii) on-line localization procedure based on the computed mappings.

4.1. Mapping Procedure

The mapping procedure is performed off-line. It is initiated by acquiring sensor output data and generating part pose error estimates, necessary to calibrate the part pose. Note that these data are obtained while the part is grasped by the robot. Then, from these calibration data, the best-fit mapping between the part pose errors and the sensor measurements is computed.

STEP 1. Acquisition of Part-Sensor Calibration Data: As described in Section 2, with reference to the coordinate frames shown in Figure 1, first, define the part frame *p-xyz* and the tool frame *t-xyz* such that they coincide with the desired location, part mating frame *2-xyz*. Adjust the placement of the sensors, such that the part at the desired location falls well within the measurable range of the

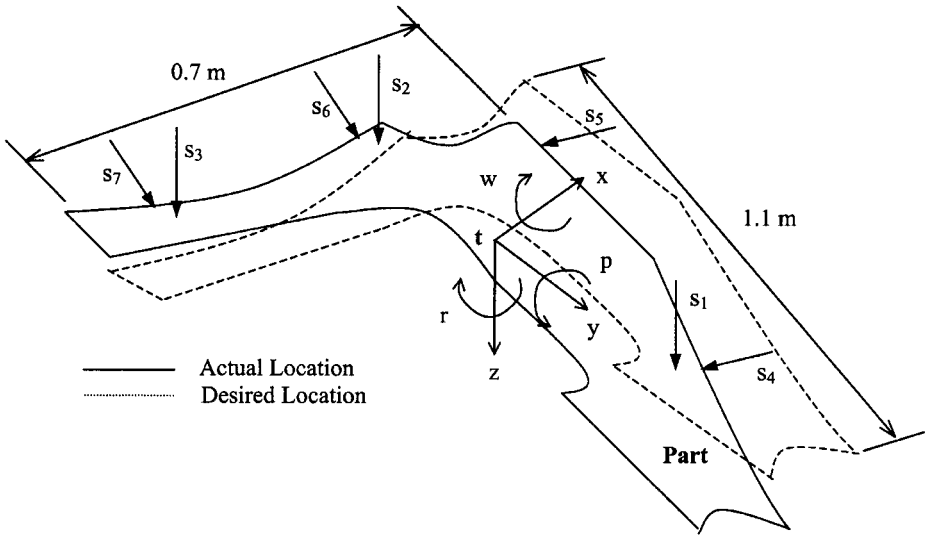


Fig. 5. Placement of measurement points.

https://doi.org/10.1017/S026357470100337X Published online by Cambridge University Press

sensors. Then, perturb the pose of the part by known amounts from the desired location while a set of measurements is taken at each selected location. Generate a set of k measurements of different part poses such that they evenly span the region around the desired location, and cover the possible part pose error range. Define $\Delta\mathbf{L}_i^p \in \Re^{1\times 6}$ ($i=1, \ldots, k$) as a vector of the perturbed part pose error, with its components identical to that in equation (1). Also, referring to equation (10), let $\mathbf{S}_i \in \Re^{1\times 7}$ ($i=1, \ldots, k$) be the corresponding perturbed measurement vector. Then, define a set of part-sensor calibration data matrices, $\Delta\mathbf{L}_C^p$ and $\mathbf{S}_C$, as

$$\Delta\mathbf{L}_C^p = \begin{bmatrix} \Delta\mathbf{L}_1^p \\ \vdots \\ \Delta\mathbf{L}_k^p \end{bmatrix} \text{ and } \mathbf{S}_C = \begin{bmatrix} \mathbf{S}_1 \\ \vdots \\ \mathbf{S}_k \end{bmatrix}. \tag{11}$$

STEP 2. Determination of Mapping: The best-fit mapping between $\Delta\mathbf{L}_C^p$ and $\mathbf{S}$ is established using the calibration data, $\Delta\mathbf{L}_C^p$ and $\mathbf{S}_C$. A process mapping, which maps the part pose error data to the measurement data, is formulated from the above set of data. Then, by applying a second-order polynomial multiple regression model, the mapping can be estimated. Define the mapping process as

$$\Delta\mathbf{L}_C^p = \overline{\mathbf{S}}_C \cdot \mathbf{M} \tag{12}$$

where $\mathbf{M}$ is the 36×6 mapping matrix and $\overline{\mathbf{S}}_C$ is a set of 1×36 augmented measurement vectors given by

$$\overline{\mathbf{S}}_C = \begin{bmatrix} \overline{\mathbf{S}}_1 \\ \vdots \\ \overline{\mathbf{S}}_k \end{bmatrix} \tag{13}$$

where:

$$\overline{\mathbf{S}}_i = [1 \quad s_1 \quad \ldots \quad s_7 \quad s_1^2 \quad s_1 s_2 \quad \ldots \quad s_1 s_7 \quad s_2^2 \quad s_2 s_3 \quad \ldots \quad s_7^2]_i \tag{14}$$

for $i=l, \ldots, k$. When $k > 7$, equation (12) represents an over-determined set of linear equations which can be solved for $\mathbf{M}$.

4.2. *Part Pose Estimation*

The part pose estimation procedure is performed in real time, as the robot moves through a simulated part mating process. During the localization of an arbitrarily placed part, the part pose error $\Delta\mathbf{L}^p$ is determined from the sensor measurements $\mathbf{S}$ using the mapping matrix, $\mathbf{M}$, computed from the mapping process.

Once an arbitrarily placed part is grasped by the robot from the part-holder, sensors take one set of measurements to construct $\mathbf{S}$, the measurement vector, given in equation (14). Then, applying the same reasoning and formulation of the mapping process expressed in equation (16), we estimate the pose error of the part, using

$$\Delta\mathbf{L}^p \approx \Delta\hat{\mathbf{L}}^p = \overline{\mathbf{S}} \cdot \mathbf{M} \tag{19}$$

where:

$\Delta\hat{\mathbf{L}}^p \equiv 1\times 6$ initial estimate vector of the part pose error $\Delta\mathbf{L}^p$,

$\overline{\mathbf{S}} \in \Re^{1\times 36} \equiv 1\times 36$ augmented measurement vector of $\mathbf{S}$,

in which the components of $\overline{\mathbf{S}}$ are defined in equation (18). The part pose measurement system is shown is shown in Figure 6. See Park and Mills[6] for detailed description of the measurement system.

5. EXPERIMENTAL RESULTS

To demonstrate the validity of the proposed technique, an experimental evaluation using the robot and part pose measurement systems was carried out. The experiment is a simulated mating process which involves a single FANUC S–110 robot manipulating an automotive front quarter panel, as shown in Figure 6. The dimensions of the quarter panel were shown in Figure 5.

Automotive body dimension tolerances require that the quarter panel to be positioned within a positional accuracy on the order of ± 0.5 mm.[1] The corresponding orientational accuracy can be obtained by assuming that the edges of the part can be displaced up to the maximum positional specification (i.e., ± 0.5 mm), which was calculated to be $\pm 0.07°$.[6] The localization of the part and correction of the part mis-location is carried out in two steps: (i) Robot calibration: estimation and correction of the robot pose error $\Delta\mathbf{L}^r$ and (ii) Part-sensor calibration: estimation and correction of the part pose error $\Delta\mathbf{L}^p$.

Robot Calibration: With the robot pose measurement system in place, two pose measurements of the S–110 robot were performed sequentially for the experiment: pose "1" and pose "2". Note that here poses "1" and "2" represent the robot tool frame at the part pick up and the part mating locations, respectively, as described in Section 3. The pose variables were obtained using the robot pose measurement technique introduced. The estimated robot pose error $\Delta\mathbf{L}^r$ at the part mating is shown in Table I. Thus, by jogging the robot, the tool frame was moved by $-\Delta\mathbf{L}^r$ relative to its current pose (pose "2"), thereby compensating the location error of the robot. With this compensation, the robot can be moved to precisely manipulate its tool frame to the part mating frame, *2-xyz*.

Part-Sensor Calibration: To localize the part, first the mapping matrix $\mathbf{M}$ was obtained. The part was picked up from the part-holder and moved to the part mating location. To compute the mapping matrix, an arbitrary total of $k=729$ perturbation points was obtained, by taking all combinations of the following perturbations: three points at 2 mm intervals for each of the three position coordinates and three points at 0.5° intervals for each of the orientation coordinates. These combinations uniformly spanned the quarter panel pose error ranges, ± 2 mm and $\pm 0.5°$ in each position and orientation coordinates, respectively. This range was only limited by the stand-off range (15 mm) of the edge sensors. As previously discussed, pose perturbations to the grasped fender location were introduced by moving the robot tool frame by the known amounts about the quarter panel desired mating location. Note that the robot was calibrated to accurately move the tool frame (hence, the part) to the mating location by the implementation of the robot calibration step.

Once the mapping matrix was computed, using the algorithm described in Section 4, an intentional part pose error was introduced by jogging the robot (the tool frame)

https://doi.org/10.1017/S026357470100337X Published online by Cambridge University Press

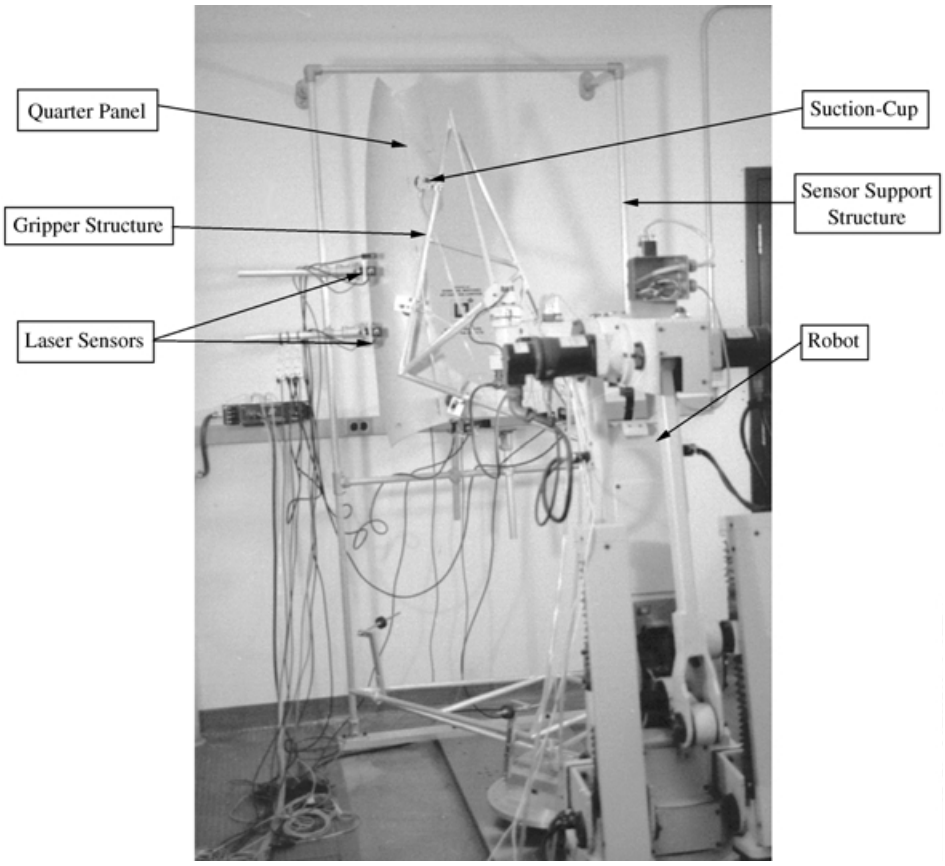


Fig. 6. Robot holding a quarter panel under part pose measurement system.

by a known amount, i.e., by $\Delta\mathbf{L}^p$=[2 mm, −2 mm, 2 mm, 0.5°, 0.5°, −0.5°], from the desired mating location. Localization of the part allows this intentional error to be compensated. The estimated part pose error, $\Delta\hat{\mathbf{L}}^p$, is given in Table II. By jogging the robot, the tool frame is moved by $-\Delta\hat{\mathbf{L}}^p$ relative to the current pose, the part pose error was compensated. Notice that the discrepancy between the true part pose error $\Delta\mathbf{L}^p$ and its estimated value, $\Delta\hat{\mathbf{L}}^p$, is very small: $\Delta\hat{\mathbf{L}}^p - \Delta\mathbf{L}^p$=[0.190 mm, −0.158 mm, −0.131 mm, 0.049°, 0.051°, −0.017°].

Obviously, however, when the robot is jogged to correct $\Delta\mathbf{L}^r$ or $\Delta\hat{\mathbf{L}}^p$, the robot cannot reposition the part more accurately than its repeatability limit, ±0.1 mm[3]. Nonetheless, the allowable localization accuracy (i.e., ±0.5 mm and ±0.07°) required in this example is much greater than the robot repeatability error and the results presented here are a good indicator that the proposed methodology works.

6. CONCLUSIONS

This paper describes a new approach for determining absolute 3-D location of parts in multi-robot assembly. It is based on a combination of two calibration procedures in order to calibrate an entire assembly system: robot pose calibration and part-sensor calibration. The proposed approach is verified through an experiment, which is a single FANUC S–110 robot simulating a mating process by

Table I. Robot pose error at mating location.

$\Delta\mathbf{L}^r$	Position Errors (mm)			Orientation Errors (°)		
	ΔX	ΔY	ΔZ	ΔW	ΔP	ΔR
Values	−1.006	0.396	−1.867	−0.544	0.213	0.149

Table II. Part pose error at mating location.

$\Delta\hat{\mathbf{L}}^p$	Position Errors (mm)			Orientation Errors (°)		
	ΔX	ΔY	ΔZ	ΔW	ΔP	ΔR
Values	2.190	−2.158	1.867	0.549	0.521	−0.517

https://doi.org/10.1017/S026357470100337X Published online by Cambridge University Press

manipulating an automotive front fender. The experiment confirrns that the proposed approach is effective and able to localize the part in all 6 DOF, within target tolerances of assembly.

References

1. J.K. Mills and J. Ing, "Dynamic Modeling and Control of a Multi-Robot System for Assembly of Flexible Payloads with Application to Automotive Body Assembly," *J. Robotic Systems*, **13**(12) (1996), 817–836.
2. J.H. Kim and H.S. Cho, "A Vision Based Error-Corrective Algorithm for Flexible Parts Assembly," *Proceedings of IEEE International Symposium on Assembly and Task Planning*. Porto, Portugal (1999), 205–210.
3. W. Xu and J.K. Mills, "A New Approach to the Position and Orientation Calibration of Robots," *Proceedings of IEEE International Symposium of Assembly and Task Planning*. Porto, Portugal (1999), 268–273.
4. R.H. McEntire, "Three Dimension Accuracy Measurement Methods for Robots," *The Industrial Robot* (1976), 105–112.
5. W. Murray and C. Pohlhammer, "Robust Estimation of the Location of a Planar Body: Results from Simulation," *ASME Journal of Dynamic Systems, Measurement and Control*, **55**(2) (1994), 1103–1109.
6. E.J. Park and J.K. Mills, "6 DOF Localization of Sheet Metal Parts in Fixtureless Assembly Scheme," *Proceedings of International Symposium on Robotics*, Montreal, Canada (2000), 344–349.
7. J.J. Craig, *Introduction to Robotics: Mechanics and Control* (Addison-Wesley, 1986).

https://doi.org/10.1017/S026357470100337X Published online by Cambridge University Press